RMP Colloquia

The onset of shear flow turbulence

Siegfried Grossmann*

Fachbereich Physik der Philipps-Universität, Renthof 6, D-35032 Marburg, Germany

Shear flow turbulence is a complex and interesting phenomenon which has been well known for a long time. The story of the physical understanding of its onset is a marvellous and recent tale of a unique nonlinearity. It is the convection term $(\mathbf{u}\cdot\nabla)\mathbf{u}$ in the equation of motion which rules the transition to turbulence by introducing a subtle interplay between the nonnormal bunching of flow perturbations and their nonlinear interaction. By nonnormal coupling to the basic laminar flow, those disturbances which are misfit to the eigendirections can transiently draw energy from the laminar shear flow and grow before they ultimately fade away. If their intermediate growth is strong enough, they interact nonlinearly. This interaction recreates new misfit flow amplitudes, which again start drawing energy, grow transiently, interact, etc. This feedback loop is able to sustain a flow which, as a consequence of the nonlinearity, is spatiotemporally deterministic and irregular at the same time. We call this flow turbulent. The feedback mechanism has to be contrasted to that of a common instability. The laminar flow stays linearly stable, all eigenvalues have negative, damping real parts. That is, laminar shear flow passes to turbulence without (linear) instability. The onset of turbulence is the nonnormal-nonlinear performance of many degrees of freedom and not merely of a single, unstable one. Both features are mediated by the convective nonlinearity.

CONTENTS

I. THE PHENOMENON AND THE PROBLEM

Turbulent flow is ubiquitous. For example, observe with fascination the dancing snowflakes in a winter storm, or the dust and tumbling paper sheets in the whirling wake of rapidly bypassing trucks, or the roaring sound of a calcified water pipe with a wide-open faucet, etc. Fast flow of air or water becomes turbulent, i.e., an irregular, time-dependent, chaotic-looking eddy flow, in contrast to the smooth, slowly creeping, laminar flow with usually a very simple velocity profile. The transition from the laminar to the turbulent state happens if the transverse momentum exchange by molecular transport, whose velocity is ν/l, can no longer compete in a sufficiently effective manner with the advective transport, whose velocity is of order U, the characteristic velocity difference across the shear. Here, ν is the kinematic viscosity of the fluid, typically of order 1 $\mathrm{mm^2\,s^{-1}}$ through 10 $\mathrm{mm^2\,s^{-1}}$ and l is the characteristic transverse length scale of the flow, e.g., the pipe radius, the distance between the atmospheric jet and the ground, etc. Transverse advection thus arises if $U \gg \nu/l$. The dimensionless quantity $U/(\nu l^{-1})$, the Reynolds number

$$Re = Ul/\nu, \tag{1}$$

becomes large, typically exceeding a value of about 1500 through 2000 for wall-bounded flow. Such numbers depend, of course, on the precise definition chosen for U and l. Here U is always understood as the largest characteristic velocity difference provided by the boundary conditions and l as the corresponding distance.

Textbook examples include shear flows with wider or smaller gaps between two planes (cf. Fig. 1), and the sensitive, irritable flame of an (old fashioned!) Bunsen burner, indicating the two modes of flow through a gas pipe (cf. Fig. 2). Shear-driven flow, denoted as Couette flow, and pressure-driven flow, so-called Poiseuille flow (in plane or circular geometry), are among the most common flows which show this onset of turbulence, technically, in a lab, or in devices (wind tunnels). I have these flows in mind for this Colloquium.

The most simple, naive idea about the two modes of fluid flow is that at low Re the laminar one is stable, but loses its stability for large enough Re, and then the turbulent one takes over. This idea has prompted in the last century the development of stability theory—more precisely of linear stability theory—connected with the names of Rayleigh (1880, 1887), Reynolds (1883), Orr (1907), Sommerfeld (1908), Taylor (1923), Heisenberg (1924) and others (cf. the textbooks by Chandrasekhar,

*Electronic address: grossmann@physik.uni-marburg.de

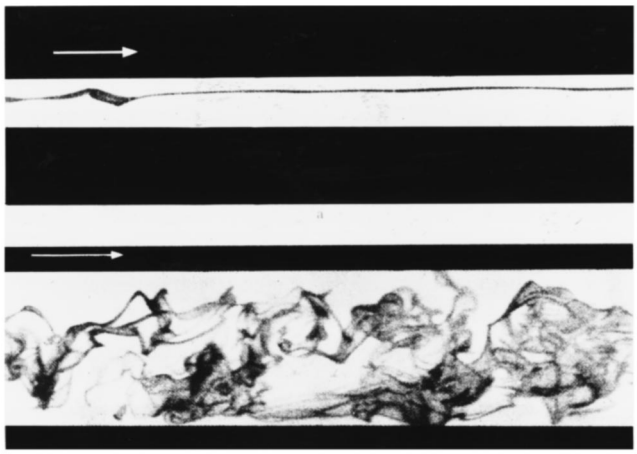

FIG. 1. Reynolds' experiment with dye injection. Upper: smooth laminar flow in the small gap of width l between two plane plates, the upper plate being sheared with the velocity U relative to the lower one. Lower: the spatially and temporally irregular turbulent flow if the gap is wide enough (gap width l large enough). From Schlichting (1959).

1961; Landau and Lifschitz, 1991; Drazin and Reid, 1981). In particular, one is reminded of Taylor's impressive success in explaining the roll formation in circular Couette flow, of the quantitative explanation of the Rayleigh-Bénard instability (Rayleigh, 1916) with its hexagon or roll patterns, of van Kármán vortices as well as of several other flow instabilities. The recent most fascinating advances are the ideas about whole series of successive instabilities, such as Landau's quasiperiodic route to turbulence (Landau, 1944; Hopf, 1948; Landau and Lifschitz, 1991), the possibility of a few-step route to chaos by Ruelle and Takens (1971), or the period doubling scenario (Grossmann and Thomae, 1977; Feigenbaum, 1978; Coullet and Tresser, 1978). All this is in the spirit of instability or repeated instability theory.

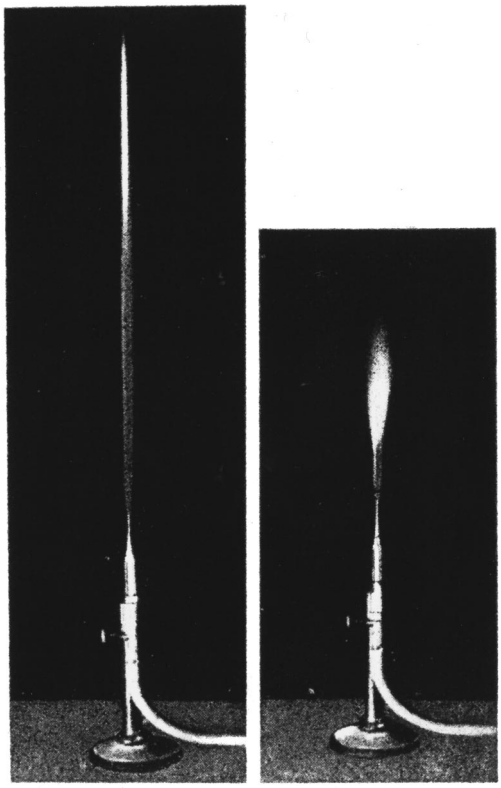

FIG. 2. Sensitive flame, laminar (left) or turbulent (right), as triggered by clapping your hand, by hissing with your mouth, by rattling a bunch of keys, or the like. One has to use an old fashioned Bunsen burner without flame rebound protection. From Pohl (1962).

Its basic feature is the discussion of the spectrum of eigenvalues $\{\lambda\}$, which describes the temporal behavior of sufficiently small disturbances of the laminar flow $\mathbf{U}(\mathbf{x})$ by

$$\delta\mathbf{u}(\mathbf{x},t)=e^{\lambda t}\mathbf{v}_\lambda(\mathbf{x}). \tag{2}$$

Let us, for example, consider such spectra for disturbances of Taylor-Couette flow. This is the flow in the gap between two concentric, independently rotating cylinders of radii r_1 and r_2 and the gap width $d=r_2-r_1$. Let the inner cylinder rotate with the angular velocity ω_1 and the outer one with ω_2, corresponding to the inner and the outer cylinders' Reynolds numbers $R_1=\omega_1 r_1 d/\nu$ and $R_2=\omega_2 r_2 d/\nu$. These Reynolds numbers $R_{1,2}$ are the external control parameters of the Taylor-Couette flow. An experiment with co-rotating cylinders is described by positive R_1 and also positive R_2, while counter-rotating cylinders have (besides the always, by definition, positive R_1) a negative R_2.

A set of spectra of this system for various chosen values of the control parameters is offered in Fig. 3. The crossing of the real part λ_r of an eigenvalue to the right of the imaginary axis indicates conventional instability by exponential growth of the corresponding disturbance. For co-rotating cylinders the transition line is, in essence, given by the Rayleigh line $R_1=(r_2/r_1)R_2$. For counter-rotating cylinders the transition line approaches a curve which exhibits the scaling behavior $R_1\propto|R_2|^{3/5}$ (Esser and Grossmann, 1996).

But, can one imagine that despite increasingly steeper shear of the laminar flow profile for increasingly faster $|R_2|$, co- or counter-rotating, at fixed R_1, the laminarity of the flow is preserved? Indeed, already Couette (1890) found turbulence in the regime of linear stability. More extended observations by Coles (1965) of the flow between counter-rotating cylinders, but also for strongly co-rotating ones, confirmed this observation (see Fig. 4). A similar situation occurs in pipe flow, in plane shear flow, etc. The spectra typically look like the pipe flow spectrum in Fig. 5. Although completely eigenvalue-stable, all real parts having $\lambda_r<0$, in all subspaces $[m|\beta]$, the flow becomes turbulent. As usual m denotes the azimuthal and β the axial wave numbers characterizing the invariant subspaces which arise because of the rotational and the translational symmetry of the geometry; we have $\delta\mathbf{u}\propto\exp(im\varphi+i\beta z/l+\lambda t)$. Since the spectra do not change their characteristic fingered structure with increasing Re, the transition to turbulence is not even accompanied by a visible signature in the spectrum $\{\lambda\}$.

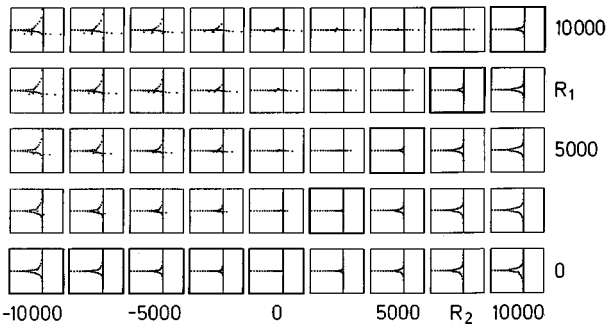

FIG. 3. A collection of eigenvalue spectra of perturbed Taylor-Couette flow between concentric cylinders. The abscissa shows the real parts, the ordinate the imaginary parts of the eigenvalues λ. The azimuthal and axial wave numbers, reflecting azimuthal and axial symmetry, are fixed to $m=0$ and $\beta=\pi$. From left to right the rotational speed $R_2=\omega_2 r_2 d/\nu$ of the outer cylinder is growing, from lower to upper the inner cylinder rotates faster, $R_1=\omega_1 r_1 d/\nu$. Here $d=r_2-r_1$ is the gap between the inner radius r_1 and the outer one r_2. The radius ratio was chosen as $r_1/r_2=0.9$. If the outer cylinder is at rest, i.e., $R_2=0$, the laminar flow profile induced the inner cylinder rotation becomes unstable at $R_{1,c}=132.7$ for this radius ratio. The Taylor vortices emerge if one eigenvalue λ has crossed the imaginary axis. Increasing $R_2>0$ at fixed R_1 stabilizes the laminar profile. Counter-rotation of the outer cylinder with respect to the inner one, with increasingly negative R_2, implies a shrinking of the unstable inner strip within the gap between the inner cylinder and the nodal surface at which the velocity profile has its zero. Because only the flow in this strip can become unstable, faster counter rotation also stabilizes laminarity at given R_1. No eigenvalue is to the right of the imaginary axis. All this is reflected also in spectra with other m and β, cf. Gebhardt and Grossmann (1993). One can identify where the borderline of linear stability will be: this line separates spectra which have one or more eigenvalues to the right of the imaginary axis from those spectra whose eigenvalues are all to the left of it, indicating linear stability.

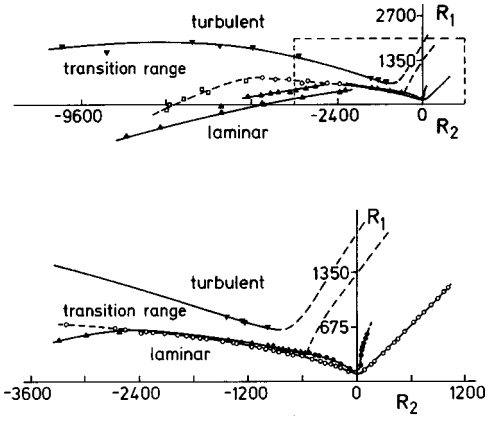

FIG. 4. The measurements by Coles (1965) show that one can observe turbulent flow in the range where all eigenvalues have negative real parts. Hence turbulence occurs although the laminar fluid flow is linearly stable. The lower diagram is an extended version of the box region in the upper diagram. The radius ratio is $r_1/r_2=0.881$.

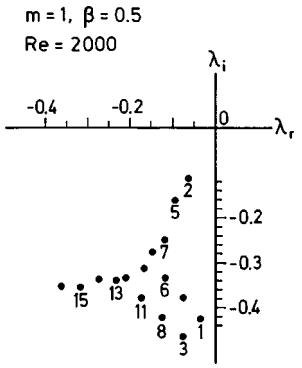

FIG. 5. The spectrum of eigenvalues λ (Brosa and Grossmann, 1999a; Boberg and Brosa, 1988) (expressed in multiples of ν/a^2) describing disturbances $\mathbf{v}_\lambda(\mathbf{x})$ of the parabolically profiled laminar Hagen-Poiseuille flow through a pipe with radius a, in the subspace $m=1$, $\beta=0.5$ of fixed azimuthal and axial wave numbers of the eigenfunctions. The λ's are labeled according to increasing damping. Towards the left, the wave length of the disturbance becomes shorter, so viscosity dominates via $\nu\Delta\mathbf{v}_\lambda\approx-\nu k^2\mathbf{v}_\lambda$. The two branches of the λ's show the influence of the advection or coupling to the laminar flow, i.e., of $(\mathbf{U}\cdot\nabla)\mathbf{v}_\lambda+(\mathbf{v}_\lambda\cdot\nabla)\mathbf{U}$ in the equation of motion. If $\mathbf{v}_\lambda$ is localized near the wall, it moves very slowly downstream, and thus its imaginary part λ_i is small. If it is localized in the center, it moves with the Hagen-Poiseuille velocity $U_0=0.25[(p_2-p_1)/L]a^2/\nu$, proportional to the kinematic pressure drop $(p_2-p_1)/L$ along the pipe of length L, therefore $|\lambda_i|$ is large. The viscous modes move with a medium velocity. What happens if *Re* is increased by the experimentalist? The wall modes are hardly influenced, the center and the viscous modes are faster (i.e., lower in the λ plane). The merging point of the branches moves down and to the left. All these features can and have been observed also in many spectra of Taylor-Couette flow disturbances (Gebhardt and Grossmann, 1993).

We have to conclude—and this is the onset-of-turbulence problem in Couette or Poiseuille flow—that the laminar-to-turbulent transition is not the consequence of a linear instability of the basic laminar flow as reflected in the crossing of an eigenvalue over the imaginary axis. We cannot expect disturbances to grow exponentially. What, then, is the physical mechanism which drives a laminar flow into turbulence? This question of deceptive plainness is the topic of this Colloquium.

II. UNSTABLE WITHOUT (LINEAR) INSTABILITY

The transition from laminar to turbulent in shear flows may be described by several generic features.

- Turbulence comes violently, unsteadily, fully, and has many scales immediately.
- To start turbulence, an initial disturbance of the laminar flow with finite strength is necessary.
- The transition has no reproducible, sharp, "critical" Reynolds number, as would be characteristic for a linear instability. The Reynolds number where the transition happens depends on the type and form as well as on the level of the disturbance.

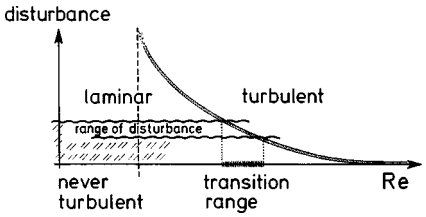

FIG. 6. Schematic plot of the double threshold for the transition to turbulence in shear flows. Since the form and the type of the disturbance—more or less misfit—is relevant, the double threshold or transition line between laminar and turbulent flow should be interpreted as the envelope of all lines for all possible types of disturbances. The exponent γ for the scaling of this threshold line $\|\delta\mathbf{u}\| \propto Re^{-\gamma}$ for large Re is expected to be 1 or slightly larger, as discussed later. For a fixed type of disturbance, as a function of only one strength parameter, the threshold seems to be fractal (Eckhardt and Mersmann, 1999), but this is not resolved in this figure. The range of typical disturbance amplitudes in an experiment implies a range of Reynolds numbers in which the transition to turbulence typically occurs.

•The onset of turbulence has a double threshold: both the initial disturbance, measured e.g., by its energy $E_{\rm dist}(0)$ or its amplitude (or norm) $\|\delta\mathbf{u}\| = \sqrt{E_{\rm dist}(0)}$, and the Reynolds number Re have to be large enough; the disturbance needed is the smaller the larger the Reynolds number already is and vice versa (see Fig. 6).

•The phase space dimension D_H, i.e., the number of degrees of freedom to describe the flow after onset, is large immediately. This gives us a hint that a too restricted number of degrees of freedom will not properly model the action of the nonlinear dynamics of the Navier-Stokes equations.

•There is an indication that the turbulent fluctuations are transient only (Brosa, 1989), but their lifetimes increase with Re so strongly that the eventual decay cannot be measured experimentally (as the disturbance leaves the pipe before decay) nor calculated numerically (its decay is beyond the length of the runs).

While pipe flow usually becomes turbulent if Re exceeds a value of about 2000, in various experiments in which disturbances of the laminar flow could carefully be avoided or considerably reduced, the onset of turbulence was delayed to Reynolds numbers up to $Re = O(10^5)$ (cf. Wygnansky and Champagne, 1973).

In contrast to Poiseuille pipe flow, which is linearly stable for all Re, in Poiseuille channel flow a critical Reynolds number of linear instability exists (Lin, 1945a, 1945b, 1946; Orszag, 1971; Orszag and Kells, 1980), $Re_c = 5772$. But the experimentally realized laminar flows usually "do not wait" until Re_c but become turbulent already at about $Re \approx 1000$. This shows particularly strikingly that the onset-of-turbulence mechanism in this flow must be different from an eigenvalue instability.

Couette channel flow shows onset of turbulence at Re of about 1300. A complete double threshold has been demonstrated experimentally for a certain type of disturbances by Dauchot and Daviaud (1994, 1995) (see also Bottin *et al.*, 1998). No linear instability is known for this flow. (Note that the Reynolds number of this flow is defined in this Colloquium with U as the relative velocity between the plates and l as their distance. Often $\frac{1}{4}$ of this Re is used, if the plates are sheared against each other, referring to the shear velocity relative to the neutral plane in the middle and its distance from either plate.) In the counter-rotating Taylor-Couette system the onset of turbulence occurs at somewhat larger Re, about 3000, indicating that the curvature of the geometry seems to suppress the onset of turbulent convection. This feature can be explained as an effect of reducing the nonnormality by the centrifugal forces (Gebhardt and Grossmann, 1999).

There is an impressive amount of important and interesting work to explain the onset of turbulence using the notions of stability theory, like (exponential) instability, subcritical transition, amplitude equations, unstable profiles, primary (linear) instability—secondary flow—secondary (linear) instability, and more. A most recent comprehensive survey of the corresponding references is available in Monin and Yaglom (1999), who cite review articles or original work by, e.g., Herbert (1988), Bayly *et al.* (1988), Orszag and Kells (1980), Orszag and Patera (1980, 1983), as well as experimental work, such as, e.g., by Nishioka *et al.* (1975), and many others. The present Colloquium develops another viewpoint for understanding the onset of turbulence in shear flows.

III. NONNORMALITY, A LINEAR STEP TOWARDS TURBULENCE

In order to identify the mechanism—different from exponential linear instability—by which the laminar flow becomes turbulent in the shear flows of interest, let us analyze the equation of motion. The Navier-Stokes equation for incompressible flow reads as

$$\partial_t \mathbf{u} = -(\mathbf{u}\cdot\nabla)\mathbf{u} - \nabla p + \nu\Delta\mathbf{u}. \tag{3}$$

Here $\mathbf{u}(\mathbf{x},t)$ is the velocity field at any position $\mathbf{x}$ and time t, and $p(\mathbf{x},t)$ is the kinematic pressure, i.e., the physical pressure divided by the constant mass density ρ. Let $\mathbf{U}(\mathbf{x})$ again denote the laminar flow, satisfying the physical boundary conditions and solving Eq. (3). We allow for a deviation $\delta\mathbf{u}(\mathbf{x},t)$, i.e., the total velocity field is $\mathbf{u}(\mathbf{x},t) = \mathbf{U}(\mathbf{x}) + \delta\mathbf{u}(\mathbf{x},t)$. The flow deviation, using Eq. (3), then satisfies

$$\partial_t \delta\mathbf{u} = -(\mathbf{U}\cdot\nabla)\delta\mathbf{u} - (\delta\mathbf{u}\cdot\nabla)\mathbf{U} - \text{pressure terms} + \nu\Delta\mathbf{u} + (\delta\mathbf{u}\cdot\nabla)\delta\mathbf{u}. \tag{4}$$

The pressure terms have not been detailed here: apart from their different vectorial character and their long range nonlocality, they are bilinear in the velocity fields $\mathbf{U}$ and $\delta\mathbf{u}$, like the first two terms written explicitly, or quadratic in $\delta\mathbf{u}$, like the last one.

As long as $\delta\mathbf{u}$ is sufficiently small, the last, quadratic term can be omitted. The remaining linear part of Eq. (4) can be solved with the ansatz of Eq. (2), which leads to the eigenvalue problem

$$\lambda\mathbf{v}_\lambda = L\mathbf{v}_\lambda. \tag{5}$$

Its eigenvalues λ and eigenfunctions $\mathbf{v}_\lambda$ depend on the laminar flow profile $\mathbf{U}(\mathbf{x})$ because L does so.

The next-to-last term in Eq. (4) is of the form $-\nu k^2$ in wave-number space, i.e., if $\delta\mathbf{u}\propto\exp(i\mathbf{k}\cdot\mathbf{x})$. Its contribution to the eigenvalues λ is purely dissipative, i.e., real and negative. The first term of Eq. (4) describes the advection of the disturbance with the laminar flow $\mathbf{U}$, contributing to λ an imaginary part proportional to U, given by $ikRe$. It is globally energy conserving. The second term is special: it represents the $\mathbf{x}$- and t-dependent advection of the laminar field $\mathbf{U}(\mathbf{x})$ by the perturbation $\delta\mathbf{u}(\mathbf{x},t)$ and therefore deforms the laminar velocity profile. This advection is independent of the wave number of the disturbance, but is also $\propto Re$. Most importantly, it is sensitive to the laminar shear profile $\partial_j U_i$. This matrix (∂U) is generically asymmetric. It has zeros along the diagonal and asymmetric nonzero off-diagonal entries. For example, in laminar plane Couette flow, only $\partial_3 U_1$ is nonzero and $\propto Re$, while $\partial_1 U_3=0$ (and analogously for pipe flow). This asymmetry of the shear matrix reflects the characteristic feature of the laminar profiles to vary perpendicularly to the direction of the flow and to be translationally invariant in the flow direction. By calculating the products of such a generically nondiagonal matrix with its adjoint matrix as well as that of the adjoint matrix with the original matrix one easily convinces oneself that the order of the factors in the products matters. One finds

$$(\partial U)(\partial U)^\dagger\neq(\partial U)^\dagger(\partial U). \tag{6}$$

This property of the shear matrix (∂U) is transferred to the linear operator L, which defines the eigenvalue problem (5) and of which (∂U) is one term,

$$LL^\dagger\neq L^\dagger L. \tag{7}$$

But it was precisely the commutability of L with $L^\dagger$ that could guarantee the mutual orthogonality of the eigenfunctions, as known for Hermitian and for unitary operators. Such operators with $LL^\dagger=L^\dagger L$ are called normal. The linear operator L for the time development of shear flow disturbances, in contrast, is generically nonnormal because of Eq. (7).

The distortion of the laminar flow field by the disturbance is not energy conserving. The term $\delta u_j(\partial_j U_i)\delta u_i$ may have any sign, so $\delta\mathbf{u}$ may lose energy, but may also draw energy from the laminar flow. Because all eigenvalues λ have negative real parts, any linear disturbance will lose its energy eventually. But transient gain is also possible.

It was known already to Orr (1907) that linear disturbances of a shear flow can grow for a while. The context was eigenvalue degeneracy. Several later authors reiterated and expanded on this observation (Landahl, 1980; Gustavson, 1981; Benney and Gustavson, 1981; Gustavson, 1991; Henningson, 1991; Butler and Farrell, 1992, 1993; Henningson *et al.*, 1993). It was, however, Boberg and Brosa (1988) who became aware of the systematic importance of a transient increase of small perturbations of the laminar flow by some appropriate linear mechanism. They still attributed it to the defectiveness of the eigendynamics in the neighborhood of the laminar shear flow, i.e., to the degeneracy or near degeneracy of some eigenvalues. When it turned out that such degeneracies are pretty rare in counter-rotating Taylor-Couette flow (Gebhardt and Grossmann, 1993), the old argument returned that one or some few accidental degeneracies can hardly be sufficient and responsible for triggering the transition to turbulence. It then was the enlightening paper by Trefethen *et al.* (1993) (see also Reddy and Henningson, 1993a, 1993b, 1994; Henningson, 1993), which identified the global feature of nonnormality as the essential property of the linear dynamics in the vicinity of the laminar flow to be systematically responsible for the transient growth of disturbances. This, together with the proper action of the nonlinear interactions between the temporarily finite disturbances of sufficient amplitude (Boberg and Brosa, 1988; Brosa and Grossmann, 1999a) has led to some self-contained understanding of how laminar flow can become turbulent.

Instead of giving general arguments, let me explain the consequences of nonnormality for nonspecialists. Consider the nonnormal matrix

$$L=\begin{pmatrix}\lambda_1 & Re\\ 0 & \lambda_2\end{pmatrix}. \tag{8}$$

Its eigenvalues are λ_1 and λ_2, its eigenvectors are $v_1=(1,0)^\dagger$ (already normalized) and $v_2\propto(Re/\Delta\lambda,1)^\dagger$. The size of the nondiagonal element Re can be taken as a measure of the nonnormality in this case, because $LL^\dagger-L^\dagger L=Re^2$. Increasing the Reynolds number Re (and thus the nonnormality) makes v_1 and v_2 more and more parallel. The cos of the angle ϕ they span is $\cos\phi=Re/\sqrt{Re^2+|\Delta\lambda|^2}$, implying $\phi\to0°$ for $Re\to\infty$ (and $\phi=90°$ if $Re=0$). But v_1, v_2 remain, of course, linearly independent unless there is exact degeneracy $\Delta\lambda=\lambda_2-\lambda_1=0$ (or if $Re=\infty$). Therefore any disturbance can be expanded in terms of v_1 and v_2. The expansion coefficients are of order 1 if the vector describing the disturbance points into about the same direction as the eigenvectors v_1 and v_2. But they are of order Re and thus huge, if the perturbation is nearly perpendicular to the v's. In the first case, which may be called a fit disturbance, the expansion coefficients simply decay because the amplitude factors $\exp(\lambda_{1,2}t)$ do so. In the second case of a misfit disturbance the huge expansion coefficients also shrink exponentially. But since the eigenvalues λ_1 and λ_2 are different, the coefficients decrease differently and with different phases. Then the superposition of the huge v_1 and v_2 components ceases to result in a small disturbance, as it did initially. Instead, it fails to do so more and more, with the consequence that the net disturbance starts to increase in size, until the superposition of the still large components is of the same order as the individual amplitudes. Simultaneously, the superposed disturbance is rotated towards the v_i directions. Consequently, the originally misfit flow disturbance at first grows and at the same time turns into the fit direction, until eventually it decays due to the

negative real parts of the λ's. A little algebra shows this quantitatively. By expanding the solution of the linear equation $\partial_t \delta u = L\,\delta u$ in terms of the above mentioned eigenvectors and determining the expansion coefficients in terms of the initial values, one finds that an initial disturbance $\delta u(0)=(u_1,u_2)^\dagger$ develops according to

$$\delta u_1(t)=\left[u_1+u_2\frac{Re}{\Delta\lambda}(e^{\Delta\lambda t}-1)\right]e^{\lambda_1 t},$$
$$\delta u_2(t)=u_2 e^{\lambda_2 t}. \tag{9}$$

While $\delta u_2(t)$ decreases, $\delta u_1(t)$ may transiently grow $\propto Re$ if u_2, the misfit component, is nonzero.

What is the generic feature of this simple example? The nonnormality of the linear dynamics quite generally will imply a bunching of the eigendirections. Disturbances that fit in this bundle decay. Those which misfit first grow (algebraically and proportional to the nonnormality, controlled by *Re*) and only after this transient increase do they decay.

The bunching of the eigendirections can physically be understood by the dominant role of the basic laminar flow. This carries any flow perturbation downstream, i.e., the eigenflow patterns will predominantly be oriented parallel or antiparallel to the main flow. Circular flow in the pipe or spanwise flow in the channel, on the contrary, are very misfit.

There are various confirmations of these features: (i) The phase space volume V spanned by the first ≈20 pipe flow eigenfunctions in the $[m=1|\beta=0{,}5]$ subspace decreases drastically with *Re*, namely $V\approx 0.97^{Re}$ (cf. Boberg and Brosa, 1988). For $Re=2000$, V is $O(10^{-27})$, or practically 0 instead of 1, as it was for $Re=0$. (ii) The overlap matrix $\langle \mathbf{v}_\lambda|\mathbf{v}_{\lambda'}\rangle$ of normalized eigenfunctions of counter-rotating Taylor-Couette flow has a broad strip of nonzero entries along both sides of the diagonal, cf. Fig. 7 (from Gebhardt and Grossmann, 1993), while for normal operators it would be $\delta_{\lambda,\lambda'}$. This figure shows particularly strikingly that the global property of nonnormality leads to a dramatic global effect of bunching of many eigenvectors, irrespective of some more or less accidental degeneracies. All eigenflows which are influenced by the laminar advection are affected. (iii) Pipe flow eigenfunctions indeed prefer, within the limits enforced by incompressibility, to flow downstream or upstream but hardly show azimuthal, rotational velocity components (cf. various flow patterns in Boberg and Brosa, 1988).

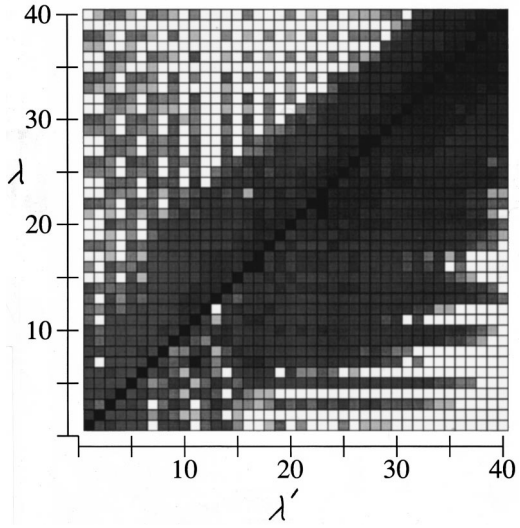

FIG. 7. The overlap matrix $\langle \mathbf{v}_\lambda|\mathbf{v}_{\lambda'}\rangle$ of the normalized eigenfunctions $\mathbf{v}_\lambda$ (λ along the ordinate) and $\mathbf{v}_{\lambda'}$ (λ′ along the abscissa) for counter-rotating Taylor-Couette flow. The upper left part of the matrix was calculated with $R_2=-10\,000$ and $[m=1|\beta=\pi]$, the lower right part with $R_2=-5000$ and $[m=2|\beta=\pi/2]$; $R_1=0$ always. The darker the entry, the larger the overlap, being between 0 and 1. For mutually orthogonal eigenvectors (as would be the case for a normal matrix) only the diagonal would be black (since $\langle v_\lambda|v_\lambda\rangle=1$), and all other entries would be white (v_λ perpendicular to $v_{\lambda'}$). Here, for Taylor-Couette flow, the nonnormality implies much overlap. Data taken from Gebhardt and Grossmann (1993).

IV. INTERPLAY BETWEEN EIGENFLOW BUNCHING AND NONLINEARITY

The generic feature of the linear dynamics in the neighborhood of the laminar flow to show nonnormal eigenflow bunching will not suffice to trigger the onset of turbulence, because ultimately any disturbance will still exponentially decay due to the negative real parts of all λ's. But if there is sufficient transient amplification, the nonlinearity can no longer be neglected. This drastically modifies the nonnormal linear dynamics.

Again, a simple argument may serve to demonstrate the subtle role of the nonlinearity $(\delta\mathbf{u}\cdot\nabla)\,\delta\mathbf{u}$. If ∇ were nothing but a vector field, the now finite disturbance $\delta\mathbf{u}$ would be mapped by the nonlinearity onto itself, apart from a numerical factor $(\delta\mathbf{u}\cdot\nabla)$. Then, because $\delta\mathbf{u}$ meanwhile has been turned into a fit disturbance, it is bound to decay $\propto\exp(\lambda t)$. But, besides transforming like a vector, ∇ is a differential operator. Therefore it probes the space dependence of the disturbance $\delta\mathbf{u}(\mathbf{x},t)$ and thus represents the direction in which the flow field $\delta\mathbf{u}$ changes, which in general is quite different from the direction into which the flow vector $\delta\mathbf{u}$ points. As a consequence the nonlinear interaction $(\delta\mathbf{u}\cdot\nabla)\,\delta\mathbf{u}$ changes—besides the magnitude—also the direction of the disturbance. One can easily convince oneself of this by considering a very simple example. Take $\delta\mathbf{u}=C(x,y)^\dagger$. Then $(\delta\mathbf{u}\cdot\nabla)\ \delta\mathbf{u}=C^2(x,y)^\dagger$, which, up to an amplification factor of C^2, is $\delta\mathbf{u}$ again. If one tries, instead, with a vortex field $\delta\mathbf{u}=C(-y,x)^\dagger$, the nonlinearity maps this onto $(\delta\mathbf{u}\cdot\nabla)\ \delta\mathbf{u}=-C^2(x,y)^\dagger$, which is not only amplified ($\propto C^2$ as before) but is also of different vectorial character. The result of the interaction is even perpendicular to the original $\delta\mathbf{u}$.

We conclude that, depending upon the spatial structure of the transiently grown disturbance, fed by the basic laminar flow as the external energy source via nonnormal coupling, a disturbance may, at least in part, be rotated into the misfit direction again, thus giving rise to another perturbation, which can draw energy anew.

By this combined effect of bunching and nonlinearity a positive feedback loop is established: small misfit disturbance → nonnormal transient amplification → nonlinear interaction → partial recreation of a misfit field → further transient growth, etc.

As models show, this feedback loop, implying algebraic and not exponential growth in general, can be very effective, and, depending on the nonnormal growth rate and ability to draw sufficient energy to supercede the losses by dissipation, can even lead to an infinite amplification. The opposite is also possible: if the number of energy-providing, misfit modes is too small in comparison to a great number of dissipating, fit modes, the feedback loop will be too weak and any disturbance will fade away. In the complete Navier-Stokes dynamics there seems to be a proper balance between the two types of mode sets, the energy-providing and the energy-consuming ones, and the feedback loop is able to sustain irregular, turbulent fluctuations.

That the full dynamics induces an irregularly fluctuating velocity field $\delta\mathbf{u}(\mathbf{x},t)$ has to be expected because the equations are nonlinear. But, moreover, the dimension D_H of the phase space involved generically must be pretty large. The reason is that nonnormality and nonlinearity cannot cooperate directly, infinitesimally, but only successively. The bunched modes within the subspaces $[m|\beta]$ of fixed symmetry with respect to azimuthal rotation (whose wave number is m) and axial translation (with wave number β) have no mutual interaction via nonlinearity. This is due to the selection rules for the quadratic nonlinearity,

$$m_1+m_2=m_3 \quad \text{and} \quad \beta_1+\beta_2=\beta_3. \tag{10}$$

Here 1 and 2 label the modes which interact by the convective Navier-Stokes nonlinearity and 3 denotes the resulting mode. Interaction thus takes place between modes or results in modes of at least two or even three different symmetry classes. But modes from different $[m|\beta]$ classes are normal to each other, since modes with different m, β are automatically mutually orthogonal.

We conclude that several different $[m|\beta]$ symmetry classes must be involved in the feedback loop in order to provide interaction as well as sufficiently many modes within each $[m|\beta]$ to provide bunching. Nonnormal bunching is necessary for the transient growth of misfit flow disturbances. The interaction is needed to enable sufficient directional redistribution of grown-up disturbances. Both requirements together easily lead to a number of modes or a phase space dimension, which is $D_H \geqslant O(100)$, in contrast to the much smaller D_H near an instability transition, where only the unstable eigenmode and its symmetry-degenerate brethren are important.

The feedback loop needs finite (instead of infinitesimal) time, because transient amplification is a necessary ingredient, and this takes time.

If this and the other time scales as well as the maximum amplification all scale with the nonnormality, $\propto Re$, one can formulate the above-mentioned feedback condition quantitatively, leading to a value for the double threshold scaling exponent γ, as first suggested by Trefethen *et al.* (1993). Start with a misfit disturbance $\sim\delta u$, have then transient maximum amplification $\sim Re\,\delta u$ followed by nonlinear interaction $\sim(Re\,\delta u)^2$ during average time $\sim Re$, resulting in another misfit disturbance $\sim(Re\,\delta u)^2 Re$. If this is larger than the original δu, the feedback loop will imply growth. Now, we have noted that the advective contribution $(\mathbf{U}\cdot\boldsymbol{\nabla})\delta\mathbf{u}$ in Eq. (4) also contributes $\propto Re$, but on the diagonal. This leads to a saturation of the nonnormal bunching and thus of the maximum amplification $\propto A\,\delta u$, with some (large) constant A. The feedback loop growth condition then is

$$(A\,\delta u)^2 Re \geqslant \delta u, \qquad \text{implying} \quad \delta u \geqslant c\,Re^{-\gamma} \ \text{with} \ \gamma=1. \tag{11}$$

Such a value for γ, was first advanced by Trefethen *et al.* (1993), and slightly larger ones have been obtained by various other authors (Butler and Farrell, 1992, 1993; Lundbladh *et al.*, 1993; Reddy *et al.*, 1993, 1998; Eckhardt and Mersmann, 1999; Chapman, 1999) by numerical analysis of the Navier-Stokes equation. Experimental values have also appeared, see, e.g., Dauchot and Daviaud (1994, 1995), Tillmark and Alfredsson (1992). The present values of γ will be given in Sec. VI.

We conclude with a final observation. Because all the components involved in the superposition of the D_H modes have a decaying exponential in front, one cannot exclude—if the deterministic-chaotic feedback loop does in some short moment not properly keep its intricate balance—that the turbulent solution fades away. Turbulence then will be of a transient nature (Brosa, 1989; Eckhardt *et al.*, 1998, 1999).

V. DEMONSTRATION OF THE NONNORMAL-NONLINEAR TRANSITION MECHANISM

Having described the basic ideas on how turbulence can be imagined to start in shear flows despite linearly stable laminarity, let me now demonstrate the validity of this mechanism by two examples: A low dimensional model system with a most general second-order nonlinearity and a Navier-Stokes-based flow with as few modes as necessary to retain all relevant features of the Navier-Stokes dynamics.

A. Two-mode model of the onset of turbulence

Let us first look at a very simple model to mimick the time evolution of a flow disturbance. We describe the deviation from laminar flow by only two mode amplitudes, $u_t=[u_1(t),u_2(t)]$, each one complex. Thus the number of degrees of freedom is $D_H=4$. Their nonnormal linear dynamics is constructed in keeping with the general ideas discussed above. For their interaction, the most general quadratic form in the components u_1 and u_2 is taken, restricted only by demanding that the equation of motion conserves energy and generates chaotic dynamics in at least some range of the Reynolds

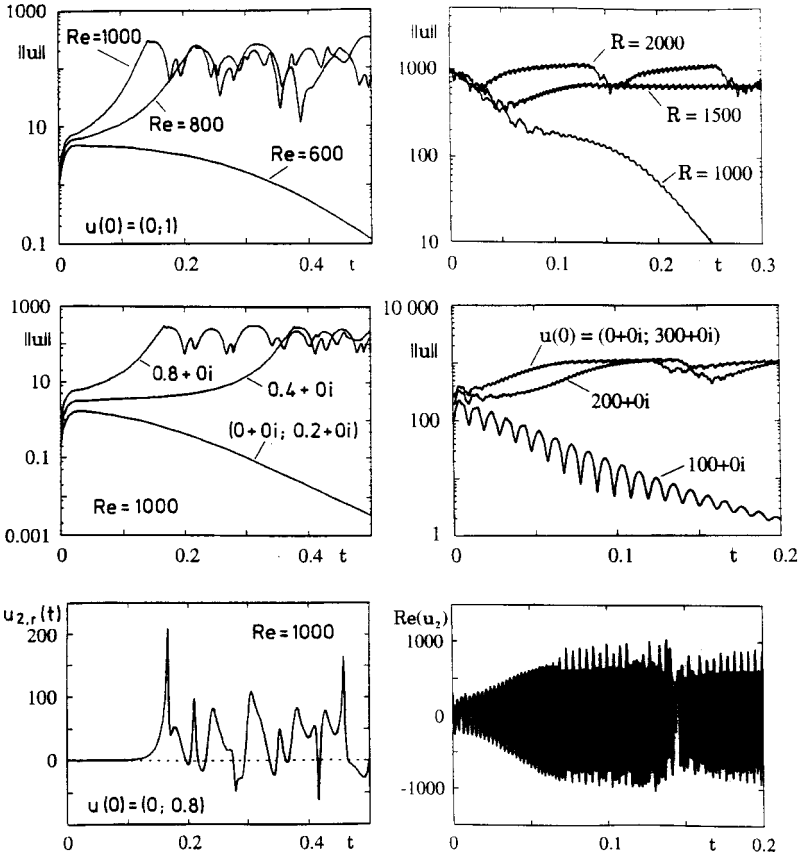

FIG. 8. Left column, upper: Time development of the amplitude $\|u_t\|$, starting from the initial disturbance (0,1), for different Reynolds numbers *Re*. Streamwise homogeneity of the disturbance, i.e., $k_x=0$, is assumed, which amounts to skipping the imaginary diagonal terms. Middle: Same for increased initial disturbance but fixed $Re=1000$. Lower: Chaotic time dependence of the real part of one component [case of largest *Re* and $u(0)$]. Right column: From upper to lower the same as in the corresponding plot to the left, but with nonzero streamwise wave number $k_x \neq 0$, i.e., including the streamwise advection of the disturbance and the corresponding imaginary diagonal terms in *L*. For further details, see Gebhardt and Grossmann (1994).

number *Re*. We thus define the model by the following equation of motion for the two complex amplitudes (Gebhardt and Grossmann, 1994):

$$\dot{u}_t = Lu_t + B(u_t,u_t), \quad \text{with} \quad L=L_\nu+L_U. \tag{12}$$

Here the matrix L_ν stands for the dissipative operator $\nu\Delta$, and the second matrix L_U represents the nonnormal coupling to the laminar flow,

$$L_\nu=\begin{pmatrix} -18 & \\ & -38 \end{pmatrix},$$

$$L_U=Re\begin{pmatrix} 0.8i & 0.7\left(1-\dfrac{\sigma\|u\|}{1+\sigma\|u\|}\right) \\ 0 & 1.1i \end{pmatrix}. \tag{13}$$

Time is measured in multiples of $(\nu/l^2)^{-1}$. The numbers in the damping matrix L_ν correspond to the values of $\nu\Delta$ expressed in wave number space by $-\nu k^2$ of the modes with the smallest wave numbers $k^2=2\pi^2/l^2$ and $5\pi^2/l^2$. The imaginary diagonal elements in L_U represent the advection by the laminar field *U* of the disturbance ($\propto ik$), and the off-diagonal element $\propto 0.7$ mimics the distortion $(\delta\mathbf{u}\cdot\nabla)\mathbf{U}$ of the laminar flow by the disturbance. Both are $\propto Re$. The additional off-diagonal term $\propto\sigma$ is introduced to switch off the nonnormality if $\|u_t\|$ approaches $O(Re)$. For this reason we choose the value $\sigma=10/Re$ for the parameter σ. Mathematically this switchoff is necessary because without it the disturbance turns out to grow indefinitely, $\|u_t\|\to\infty$; the feedback loop simply is too effective. Physically it represents the flattening of the turbulent mean profile in the bulk, which diminishes the mean shear, $\partial_3\langle U_1\rangle\approx 0$, and thus no nonnormality is left in the interior of the flow volume.

The second-order nonlinearity *B* with the components B_i $(i=1,2)$ is taken in its most general form $B_i=\Sigma b_{ijl}u_j u_l$, restricted only by energy conservation $u^*B+uB^*=0$ for all *u*. We chose the matrix elements b_{ijl} to remix the components and to generate a deterministic chaotic dynamics, but they are otherwise arbitrary. No recourse to the Navier-Stokes nonlinearity $(\mathbf{u}\cdot\nabla)\mathbf{u}$ could be made under these constraints, however simple they are.

This model has been studied in detail by Gebhardt and Grossmann (1994) (see also Baggett and Trefethen (1997), where it has been compared with other low dimensional models). It gives the double threshold and other characteristic features of the nonnormal-nonlinear turbulence transition, some of which are displayed in Fig. 8.

An intuitively rather puzzling question can be answered by this simple model. The loss of energy stability in the shear flows through pipes or channels is known to happen at much lower *Re* already than the onset of turbulence. Namely, energy stability is lost at $Re=O(80)$ (cf. Joseph, 1976; Drazin and Reid, 1981), while turbulence sets in at $Re=O(1200)$ or more. How can this be compatible? How can one understand that despite the possibility that the disturbances grow in energy, turbulence does not set in?

The temporal development of small disturbances u_t is characterized by L of Eqs. (12) and (13) after setting B and σ equal to zero. This then describes the linear dynamics of the velocity field u_t. For the energy of the disturbance, measured by $\|u_t\|^2$, the relevant linear operator is $L_E = L + L^\dagger$. It is Hermitian, and its eigenvalues are real (but different from $\lambda + \lambda^*$). L_E develops a positive eigenvalue, which appears if Re exceeds $Re_{ES} = 74.7$. The puzzle now is that L_E has an eigenvalue $\lambda_E > 0$, and thus the energy $\|u_t\|^2$ can grow, but nevertheless the laminar flow is stable: Since the λ's of L all have negative real parts, u_t decays, and turbulence does not set in before $Re = O(1000)$.

To resolve this puzzle we consider the "equation of motion" for the energy,

$$\frac{d\|u_t\|^2}{dt} = \langle u_t | (L + L^\dagger) u_t \rangle = \lambda_E(t) \|u_t\|^2. \tag{14}$$

The time-dependent rate $\lambda_E(t)$ may be introduced:

$$\lambda_E(t) = \langle u_t^0 | L_E u_t^0 \rangle = \sum_a \lambda_{E_a} |\langle V_a^0 | u_t^0 \rangle|^2. \tag{15}$$

Here λ_{E_a}, $a = 1,2$, are the two energy eigenvalues, one of them negative, the other one positive beyond Re_{ES}. The set of V_a^0 are the energy eigenvectors, normalized and mutually orthogonal. u_t^0 is the normalized solution of the linearized equation of motion (11) for the field amplitude itself. It is a unit vector.

Now, initially, if $u_{t=0}^0$ is parallel to the unstable eigendirection $|V_1^0\rangle$, we have $\lambda_E(t) \approx \lambda_{E_1} > 0$. The disturbance grows. But in the course of time u_t is rotated into the fit direction. It then turns out to have equal overlap matrix elements with both (all) L_E eigenvectors (the latter forming a complete orthonormal basis). Thus the contributions $|\langle V_a^0 | u_t^0 \rangle|$ are the same for all a, and

$$\lambda_E(t \text{ large}) \sim \sum_a \lambda_{E_a} < 0. \tag{16}$$

For L defined by Eq. (12) one obtains $\lambda_E(t \text{ large}) \sim \lambda_{E_1} + \lambda_{E_2} \approx (-18 - 38 + Re) + (-18 - 38 - Re) = -112$. The large terms $+Re$ and $-Re$ cancel each other and thereby lose their dominance.

We note that energy instability and relaminarization of the flow are compatible because the (linear) flow is turned around into that very small section of the phase space which is defined by the fit eigenbundle. The eigendirections of the energy operator, spanning the phase space as a complete orthonormal basis, all have the same projections on the L eigenbundle. Therefore the unstable directions with positive λ_E are more than compensated by the stable components with $\lambda_E < 0$. It is again the bunching due to nonnormality which is responsible for this interesting mechanism.

As has been described, if the transient growth becomes strong enough, the quadratic term $\propto u^2$, i.e., the interaction of the velocity field with itself, will become sizable. This interaction drives at least parts of the disturbance, which had just been turned linearly into the direction of the eigenbundle, out of that eigendirection. This then misfit, scattered part of the disturbance now takes notice of the unstable L_E eigendirections again, grows further, etc., as explained above.

B. Mode-reduced Navier-Stokes dynamics

Let us consider now the second example. Instead of studying a model dynamics, the Navier-Stokes equation for incompressible fluid flow itself is solved. The approximation here consists in admitting a finite number of modes only, but interacting with the Navier-Stokes nonlinearity itself. In fact, we even try to reduce this number of modes as much as possible, but still can identify and demonstrate the nonnormal-nonlinear onset mechanism. For details see Brosa and Grossmann (1999a).

Because the nonnormality parallelizes those eigenflows which are sizably affected by the advection with the laminar flow rather than by the dissipation, the numerical handling of the Navier-Stokes dynamics in the basis of eigenflows becomes difficult. For example, the overlap matrix $\langle \mathbf{v}_\lambda | \mathbf{v}_\lambda' \rangle$, cf. Fig. 7, is close to being singular. More precisely, it has a large condition number, i.e., a large ratio between its largest and its smallest eigenvalue. To bypass numerical problems arising from these specific properties of the eigenflow basis, caused by the nonnormality of the linear operator L, it is useful to employ the QR decomposition of the eigenflow basis $\{\mathbf{v}_\lambda\}$ of linearly independent but nonorthogonal unit vectors in each $[m|\beta]$ subspace of fixed azimuthal and axial wave numbers m and β. Here R is an upper triangular matrix (zero entries below the diagonal) and Q is unitary. The Q eigenstates $\{\mathbf{q}_\kappa\}$ then span the $[m|\beta]$ subspace with mutually orthogonal flow patterns. These can be ordered, in addition, according to their ability to transiently being amplified, denoted as amplification quality. This notion is defined quantitatively as the ratio of the maximum energy along the linearly calculated solution to the initial energy.

The eigenstates $\mathbf{v}_\lambda$ with low labels, defined in Fig. 5, are dominated by the laminar advection and only weakly damped. As one expects, it indeed turns out that they are fit flow patterns with only poor or no transient amplification quality. Those with the high labels, in contrast, are hardly influenced by the laminar advection but are strongly damped. And since they are dominated by the $\nu\Delta\mathbf{u}$ term in Eqs. (3) and (4), which is Hermitian, they are mutually orthogonal. For both reasons they also have only bad amplification quality. Most effective in their quality of transient amplification are the modes in the palm range between the spreading fingers, the "Y" of the spectrum in Fig. 5. These states are not yet too strongly damped and they are not yet too much influenced by advection, and therefore fit less well into the bundle of fit eigenvectors with small λ. Nonnormality and transient amplification become strong for these $\mathbf{v}_\lambda$.

One can isolate the combined properties of small damping and being most misfit by performing the QR decomposition with the backward sequence

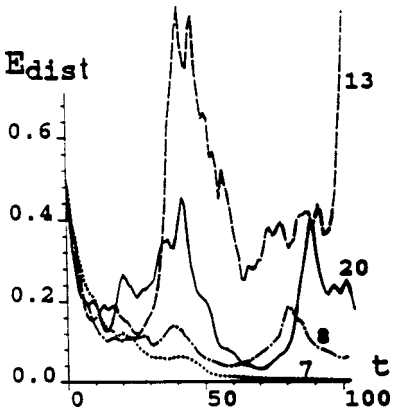

FIG. 9. Time development of the energy of the disturbance, $E_{\rm dist}(t)$. The parameters are $Re=2000$, $N=7$, 8, 13, or 20 modes per $[m|\beta]$ class, and three such communicating classes. Initial disturbance: Superposition of the least damped eigenmodes in [1|0.5] and [0|1.0]. These are fit disturbances, which decay. Their interaction produces misfit components, which are then amplified.

$\{\mathbf{v}_N,\mathbf{v}_{N-1},\ldots,\mathbf{v}_1\}$ of eigenmodes. N must not be too small. For $Re=2000$ the value of $N=20$ is convenient, the smallest possible N we could identify as leading to some noteworthy amplification quality being 8. The correspondingly ordered $\mathbf{q}$ flows $\mathbf{q}_1,\mathbf{q}_2,\ldots,\mathbf{q}_\kappa,\ldots,\mathbf{q}_N$ have decreasing damping and increasing amplification quality with growing index κ.

Next, the concept of communicating classes is introduced. These are sets of several $[m|\beta]$ classes with different azimuthal and axial wave numbers, which are connected by the interaction via the m,β selection rules (10). The smallest nontrivial communicating set of $[m|\beta]$ classes is the triple {[1|0.5], [−1|0.5], [0|1.0]}.

In Fig. 9 solutions obtained with various numbers N of modes per $[m|\beta]$ class are shown. If N is only 7 or 8 there is not sufficient transient amplification, the misfit component is too weak. If $N=13$, sufficiently many misfit modes are included and therefore sufficient transient growth occurs. But this set of modes has insufficiently many damped modes. As a result the energy even grows *ad infinitum.* If $N=20$, the energy input and the damping are balanced. The solutions calculated with this set of 3 communicating classes with chosen azimuthal (m) and axial (β) wave numbers, containing $N=20$ complex modes each, thus with $3\times20\times2=120$ real amplitudes, fluctuate long and irregularly, cf. Figs. 9 and 10.

We now can analyze some details of the nonlinear interaction in this set of modes, in order to check and to verify the validity of the picture about the onset of turbulence, which has been developed here. For instance, we observe that modes which have lost their transient amplification qualities, as, e.g., $\kappa=1$ in $[m=0|\beta=1.0]$ and $\kappa=5$ in [1|0.5], interact to give a $\kappa=8$ mode in the symmetry class [−1|0.5], which has a large potential for transient growth. In Fig. 11 this as well as another such example are offered. It gives confirmation of the partial redistribution process of the fit modes into the misfit directions by the nonlinearity.

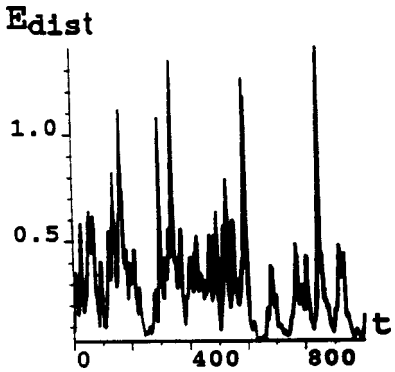

FIG. 10. Long-lasting fluctuations in the system with $Re=2000$, $N=20$, and three communicating classes.

With such about 100 well-chosen, real amplitudes, the solutions of the Navier-Stokes equation reproduce the characteristic double threshold (cf. Fig. 6). The smallest possible mode number we could find to do so comprised $3\times8\times2=48$ real amplitudes. Why are $O(100)$ real amplitudes necessary although the four-amplitude model of Sec. V.1 already showed the onset of turbulence despite stable laminarity? The reason is, in the four-amplitude model the most general interaction matrix b_{ijl} (under reasonable physical constraints only) had to be used. This most general matrix cannot be derived from the Navier-Stokes nonlinearity $(\mathbf{u}\cdot\nabla)\mathbf{u}$; on the contrary, the four-amplitude model fails, if one restricts oneself to the Navier-Stokes-generated interaction of the available amplitudes. In the Navier-Stokes-based calculations of this section more modes are needed, because the physically correct interaction is kept.

One can also calculate the corresponding flow profile, although at these still rather low Re and with so few modes this is not very firm. But the tendency of flattening the parabolic Hagen-Poiseuille flow profile in the interior of the pipe and indication of developing a steep boundary layer are already found, cf. Fig. 10 in Brosa and Grossmann (1999a).

Thus these mode-reduced Navier-Stokes solutions seem to confirm the nonnormal-nonlinear mechanism of transition to turbulence described in the previous sections.

VI. THE DOUBLE THRESHOLD SCALING

Until now we have concentrated on explaining the mechanism which leads to a double threshold for the onset of turbulence despite stable laminarity, $\|\delta\mathbf{u}\| \propto Re^{-\gamma}$. It describes the necessary size of disturbances at a given Re or the necessary Reynolds number Re at a given disturbance level to trigger the onset of turbulence. Or, stating it alternatively, the domain of stable laminarity, the basin of attraction of the laminar flow, shrinks algebraically with increasing Re.

Stable laminarity—being the subject for the Adams Prize of the University of Cambridge for 1888—in a decreasing domain with increasing Reynolds number has been described, incidentally, more than a hundred years

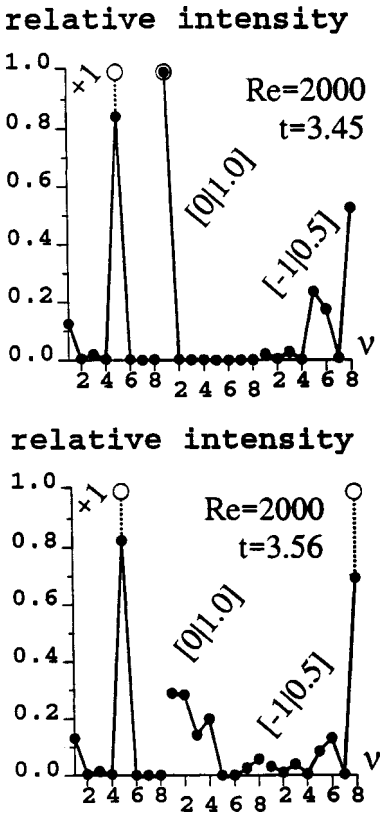

FIG. 11. Nonlinear time development of a system of three communicating classes, eight modes each, for $Re=2000$. The integration time is finite but still sufficiently small so that only about one interaction can happen. Along the abscissas each figure (upper as well as lower) shows the intensities of the eight modes in the three classes [1|0.5] (abbreviated as +1 in the graph), [0|1.0], and [−1|0.5]. The circles ○ indicate the initial amplitudes, the full dots ● the final ones after $t=3.45$. The sum of the initial as well as of the final intensities has been normalized to 1, therefore we speak of "relative intensities." Upper: Two energy consuming, fit modes, namely $\kappa=1$ in [0|1.0] and $\kappa=5$ in [1|0.5], produce misfit amplitudes in [−1|0.5] (with labels $\kappa=5$ and $\kappa=8$), which have good amplification quality. Lower: A misfit mode, $\kappa=8$ in [−1|0.5] and a fit one, $\kappa=5$ in [1|0.5] by their interaction produce low amplification quality modes, $\kappa=1$ through 4 in [0|1.0]. These are needed to create other amplitudes of high amplification quality as was just shown in Fig. 11, upper.

ago by Lord Kelvin (Thomson, 1887): "It seems probable, almost certain indeed, that analysis...will demonstrate that the steady motion is stable for any viscosity, however small; and that the practical unsteadiness pointed out by Stokes forty-four years ago, and so admirably investigated experimentally five or six years ago by Osborne Reynolds, is to be explained by limits of stability becoming narrower and narrower the smaller the viscosity." (Lord Kelvin then presented a proof for plane Couette flow.)

Meanwhile some properties of this double threshold have been clarified. As is clear from the description of the nonnormal-nonlinear mechanism, the onset of turbulence depends on the type and on the details of the triggering disturbance and not only on its strength alone. But for a fixed type of disturbance as a function of one parameter only, say the strength, the double threshold curve seems to be fractal. This was shown with reduced mode number solutions of the Navier-Stokes dynamics by Eckhardt and Mersmann (1999). The envelope of their fractal boundary between laminar and turbulent runs shows an algebraic scaling $\propto Re^{-\gamma}$ with $\gamma\approx 1$, in the range $Re\leqslant 4000$. Of course, experimentally uncontrollable fluctuations of the initial conditions will smear out too detailed fine structures of the transition curve. Nevertheless it is of interest to look to experiment for such structures in the onset range, cf. Darbyshire and Mullin (1995).

The present values of the double threshold scaling exponent γ obtained by careful numerical simulations of the Navier-Stokes equation (Lundbladh *et al.*, 1993; Reddy *et al.*, 1998) are $\gamma=1$ and $\gamma=\frac{5}{4}$ for, respectively, streamwise and oblique initial flow structures in plane Couette (shear) flow. The corresponding values for plane Poiseuille, i.e., pressure driven flow, are $\gamma=\frac{7}{4}$ in both cases of streamwise or oblique initial perturbations. Recent asymptotic analysis of the Navier-Stokes equations (Chapman, 1999), i.e., order of magnitude comparison of the relevant terms for large Re and looking for the transient amplification potential of the modes and their interaction order, led to a slightly higher double threshold, meaning smaller values for the scaling exponents, $\gamma=1$ and $\gamma=\frac{7}{6}$ for plane Couette and $\gamma=\frac{3}{2}$ and $\gamma=\frac{17}{12}$, respectively, for plane Poiseuille flows. The first values again refer to streamwise, the second to oblique initial disturbances.

The difference between the analytically and the numerically obtained scaling exponents γ was traced back by Chapman (1999) to not yet being in the asymptotic Re range numerically. There are also other cases in which one meets appreciable deviations of the numerical from the asymptotic exponents. The scaling of the present best energy-dissipation-rate bound for plane Couette flow, $\varepsilon/(U^3L^{-1})\propto Re^{-\alpha}$, may serve as an example. One finds $\alpha=0.08$ in the range up to the not at all small value of $Re\approx 10^6$, but $\alpha=0.18(1)$ asymptotically in Re (Nicodemus *et al.*, 1999; cf. Fig. 1 of that paper).

VII. LARGE PHASE SPACE DIMENSION

As was explained earlier, the intricate interplay of the nonnormal bunching and the nonlinear interaction implied by the convective nonlinearity $(\mathbf{u}\cdot\nabla)\mathbf{u}$ needs quite a number of degrees of freedom to function. The smallest we found was 48, and for longer turbulent runs, 120. But there are more and larger sets of communicating classes in the Reynolds number range, where the onset of turbulence occurs. Depending on the initial conditions, they too may contribute. And the interaction couples them. Thus it is of considerable interest to estimate how large the number of degrees of freedom near the onset of turbulence really is, i.e., how large the corresponding phase space dimension D_H has to be, and which are the physical reasons for its magnitude.

There exist rigorous upper bounds for D_H (Ruelle, 1982, 1984; Lieb, 1984). It is not yet clear to what extent these might be overestimates. One may also evaluate D_H rather directly to get an appropriate, though nonrigorous estimate (Grossmann, 1994), following Ruelle's line of argument. One uses the relation between the dimension D_H and the Lyapunov spectrum $\{\Lambda_1 \geqslant \Lambda_2 \geqslant \cdots \geqslant \Lambda_b \geqslant \cdots\}$ of the nonlinear dynamical system at hand (Kaplan and Yorke, 1979). It states that D_H is the largest number for which the sum of Lyapunov exponents ordered according to decreasing size is still positive,

$$\sum_{b}^{D_H} \Lambda_b \geqslant 0. \tag{17}$$

To calculate the Λ_b spectrum of a Navier-Stokes flow $\mathbf{u}(\mathbf{x},t)$ one has to analyze the growth rates of small deviations averaged along the actual flow. The linear operator determining the growth of $\|\delta\mathbf{u}\|^2$ is $L_E = \nu\Delta + (\nabla\mathbf{u})_{\text{sym}}$. Surely, the spectrum of the Laplacean alone is $-\nu\mathbf{k}^2$. The second term, originating from the Navier-Stokes nonlinearity and depending on $\mathbf{x}$ and t, appears to be of insurmountable difficulty. Its matrix form is $(\partial u_i/\partial x_j + \partial u_j/\partial x_i)/2$. It becomes tractable if one simplifies drastically (Ruelle, 1982) by diagonalizing it with respect to the vector indices i,j and, furthermore, by neglecting its space and time dependence by taking its mean value along the solution trajectory, thus erasing the wild field fluctuations. These two steps mean to substitute the $\mathbf{x}$, t-dependent field derivative matrix operator by the number $\sqrt{\varepsilon/2\nu}$. Then L_E becomes a diagonal multiplication operator and $\Lambda_b = \Lambda_{\mathbf{k}} = -\nu k^2 + \sqrt{\varepsilon/2\nu}$. Counting the number of $\mathbf{k} = (2\pi l^{-1})\mathbf{n}$ in the largest sphere satisfying the inequality (17), $\mathbf{n}$ having integer components, allows us to determine D_H. For more details see Grossmann (1994).

The result for the phase space dimension D_H necessary to describe a turbulent flow whose inner, viscous length scale is $\eta = (\nu^3/\varepsilon)^{1/4}$ reads

$$D_H \simeq 0.0216\left(\frac{l}{\eta}\right)^3 \simeq \left(\frac{l}{3.6\eta}\right)^3. \tag{18}$$

If the mean energy dissipation rate ε in the bulk is expressed in terms of Re via $\varepsilon = U^3 l^{-1} c_\varepsilon(Re)$, one obtains for not too small Re the constant value $c_\varepsilon \approx 0.6$ (Lohse, 1994; Grossmann, 1995). Thus omitting possible intermittency corrections, the phase space dimension of a turbulent fluid flow with Reynolds number Re reads (up to intermittency corrections) as

$$D_H \simeq 0.015\, Re^{9/4}. \tag{19}$$

In the range of small Re, one finds $c_\varepsilon = Re^{-1}$, therefore

$$D_H \simeq 0.0216\, Re^{3/2}, \quad Re \text{ small}. \tag{20}$$

Applying these expressions for D_H one finds that if the onset of turbulence happens at $Re \approx 1500$, the typical phase space dimension (number of degrees of freedom) of the curly, irregularly fluctuating flow is, using Eqs. (18) and (19), $D_H = O(10^5)$, and $l/3.6\,\eta = O(60)$. That is, $N = 20$ complex modes or 40 real ones for the radial direction is about sufficient. But the other spatial directions φ and z, characterized by the wave numbers m and β, are not yet sufficiently resolved with only three communicating classes $[m|\beta]$. One has to expect that more $[m|\beta]$ blocks have to be added if the full dynamics and observed small scale patterns near onset are to be resolved.

Note that $\eta \approx l/200$, i.e., there are indeed not only temporally but also spatially decorrelated flow fluctuations.

If a flow experiences a conventional linear instability, one typically finds $l \approx 7.5\eta$ (cf. Esser and Grossmann, 1996). Then Eq. (18) tells us that $D_H = O(9)$ and only a few degrees of freedom are involved. The corresponding Reynolds number can be evaluated according to Eq. (20) and is $Re_c = O(60)$. Indeed, Taylor-Couette flow with a rotating inner cylinder becomes unstable for $Re_{1,c} \approx 70$ for intermediate values of the radius ratio r_1/r_2. And energy instability in pipe flow and in plane Couette flow occurs at $Re = O(80)$.

The very different mechanisms of linear instability and of nonnormal-nonlinear onset are clearly reflected thus also in the number of the participating degrees of freedom. These are only a few in the former case but quite many in the latter transition mechanism.

Fully developed turbulent flow with $Re \approx 5 \times 10^6$ has, incidentally, as many as $D_H = O(10^{13})$ degrees of freedom. This seems huge but is still small in view of the infinitely many degrees of freedom for a continuous flow field. Typical inner lengths are about $\eta \approx 3$ mm, and thus the D_H density is $O(1\ \text{cm}^{-3})$.

VIII. PHASE SPACE STRUCTURES NEAR ONSET

Until now we have analyzed the mechanism for the transition to turbulence. Another interesting question is, how large on average are the amplitudes of the turbulent flow fluctuations? This question also arises, of course, for eigenvalue-unstable transitions; there it usually can be answered by including the nonlinear terms in the (Landau-type) free energy. At shear turbulence onset this question seems to find its answer in a characteristic feature of complex systems dynamics enjoying chaotic time development: In the phase space of chaotic systems there is a skeleton of periodic states, although unstable (Ruelle, 1978; Eckmann and Ruelle, 1985; Cvitanović, 1988). Chaotic trajectories can be approximated by motion on this skeleton. Consequently, if one knows these unstable periodic orbits, one will know the typical amplitudes. By unstable periodic orbit analysis one can even calculate the average properties of chaotic systems (at least of hyperbolic ones) with surprising accuracy (Cvitanović, 1988; Eckhardt and Ott, 1994; Eckhardt and Grossmann, 1994, etc.). The number of such states increases strongly with the control parameter.

It thus has to be expected that similar unstable phase space orbits are present also in turbulent flows, increasingly more so with increasing Re. The simplest ones are the period one or stationary (unstable) solutions of the dynamic equations. In fluid flow these are stationary flow patterns, which solve the time-independent Navier-Stokes equation but are different from the laminar solu-

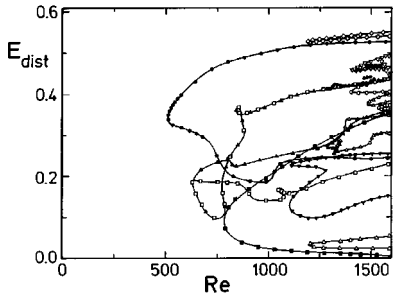

FIG. 12. The tangle of unstable stationary states, which are denoted by $\mathbf{w}(\mathbf{x})$, in the parameter space energy $E_{\rm dist}(\mathbf{w})$ versus Re, from Eckhardt *et al.* (1998) (by courtesy of Bruno Eckhardt and Armin Schmiegel, who provided this figure prior to publication). The states in this figure have been calculated with 302 (real) degrees of freedom, Fourier modes in the x and y directions, and Legendre polynomials in the z direction. Only time-independent states with a certain symmetry of the flow pattern are shown. The solid lines connect states related by a continuous deformation of their flow patterns. The symbols ●, □, etc., label different types of unstable stationary flow fields.

tion. Indeed, after a first, single, additional time-independent flow had been discovered (Nagata 1990, 1997; Clever and Busse, 1992, 1997), recently Eckhardt, Marzinzik, and Schmiegel (1998) found a rich structure of stationary Navier-Stokes solutions $\mathbf{w}(\mathbf{x})$ using a reduced (962 degrees of freedom) mode number code. In contrast to the laminar flow, which is (linearly) stable, these further states, $\mathbf{w}(\mathbf{x})$, are unstable. They are born in a saddle-node-like bifurcation when one increases the Reynolds number Re and are expected to have many unstable and also many (though fewer) stable directions in phase space. The first of these additional stationary solutions appears at $Re \approx 500$ (Re depending on the considered symmetry subclass of the flow and also on the aspect ratio of the flow's geometry). For larger Re, an increasing number of stationary solutions emerge, forming a tangle of states in the parameter plane spanned by the disturbance energy $E_{\rm dist}(\mathbf{w})$ versus the Reynolds number Re, as displayed in Fig. 12. There are indications (Eckhardt, 1999) that besides this set of time-independent states also periodic unstable states exist.

Since the unstable stationary states determined numerically are born in a saddle-node bifurcation with stable and (more) unstable manifolds, the phase point of an actual physical flow solution $\mathbf{u}(\mathbf{x},t)$ of the Navier-Stokes equation will, in the vicinity of the stationary states, be attracted in some phase space directions and repelled in others. Being repelled from one such state, it temporarily becomes attracted by another, is then repelled also there, etc. Therefore the phase point of the physical flow in the course of time travels erratically through the tangle of stationary states, whose threads attract and repel it, again and again, irregularly, until it eventually ''falls'' through the tangle and approaches the laminar state. The set of unstable stationary states thus constitutes a strange repeller in the phase space of flows. Knowing this set enables one to estimate the typical deviations of the turbulent velocity from the laminar one and also the typical amplitudes of the turbulent fluctuations about their mean. And also, the idea is obvious that the appearance of this repeller with increasing Re should indicate and be related to the first possibility of turbulent solutions by the nonnormal-nonlinear transition to turbulence. This then might answer the question for the lowest Reynolds number $Re_{\rm border}$, where the double threshold starts. Possibly the threshold curve has a pole there (cf. Fig. 6). The data seem to indicate that the scaling exponent for the approach to this asymptote is different from γ, the asymptotic exponent for $Re \to \infty$ (Dauchot and Daviaud, 1995).

The envelope to the energies of the presently known unstable stationary states plotted in their Reynolds number dependence seems to decrease algebraically with Re roughly $\propto Re^{-\gamma'}$, with $\gamma' \geqslant 1$, in the range $Re \leqslant 40\,000$ (Eckhardt *et al.*, 1998). If the suggested relation between the possibility of turbulent solutions and the stationary solutions proves to be valid, γ' should coincide with γ, the double threshold exponent.

IX. STREAMWISE FLOW PATTERNS, TWO OR THREE DIMENSIONAL?

In experiment, after the onset of turbulence, the mean flow profile changes. This has to be reproduced by the time average of $\mathbf{u}(\mathbf{x},t)$, if the time development of those flow modes is inserted, which participate when calculating the solution. In the mode-reduced Navier-Stokes dynamics (Sec. V.B) this can indeed be shown to happen (Brosa and Grossmann, 1999a). To learn even more, let me recall which modes are participating. Part of the eigenflows is oriented in the basic flow direction, i.e., streamwise. Some energy dissipating, smaller wavelength modes are also included. These dissipating modes are advected streamwise. But also misfit modes must be present; these are excited by the nonlinear interaction again and again. Such misfit modes are not dominated by the laminar advection. Instead they are wall normal and spanwise flows. One therefore expects that the onset mechanism needs three-dimensional flow perturbations.

That three-dimensional disturbances for the onset of turbulence are necessary can be confirmed explicitly within the nonnormal-nonlinear mechanism (Brosa and Grossmann, 1999b). Comparing two- and three-dimensional flow perturbations, one finds the necessary transient amplification quality only in three dimensions. Two-dimensional modes turn out to have almost zero amplification quality. One also finds that the modes which have largest qualities are streamwise oriented rolls, $k_x \to 0$, $lk_y \approx 1$. The well-known failure of two-dimensional theories, as, e.g., the Orr-Sommerfeld equation (Orr, 1907; Sommerfeld, 1908) but also later ones, thus finds its explanation in that it suppresses the possibility of transient growth by not properly admitting the nonnormal bunching of the high quality eigenfunctions in phase space.

Flow patterns which mirror these features have been considered by Waleffe, Kim, and Hamilton (1993), Wal-

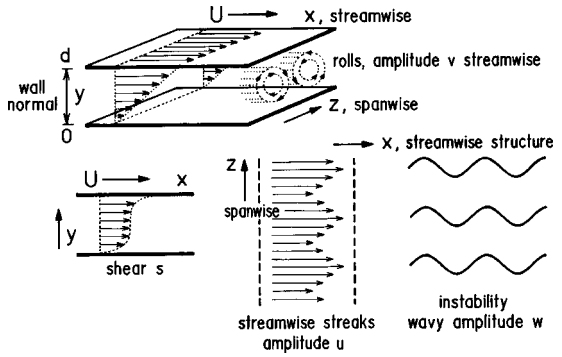

FIG. 13. Schematic plot of streamwise streaks (stripes of larger or smaller velocity, as indicated by the arrows) and rolls at the onset of turbulence in plane Couette flow. The rolls' amplitude v, together with the shear s, feed the streaks u, which in turn excite a wavy instability w, that resupports the rolls v, etc.; cf. Waleffe (1995).

effe (1995), and Hamilton, Kim, and Waleffe (1995). For a sketch of the relevant flow pattern, see Fig. 13.

Another set of illuminating results has been obtained by reduced-mode number Navier-Stokes calculations of plane Couette flow (Schmiegel and Eckhardt, 1999a, 1999b). The time development of vortex-type initial perturbations with different orientations was studied, in particular their lifetimes and the relaxation to the turbulent state. These authors also try to identify the smallest onset-of-turbulence border by adiabatically following turbulent states from larger down to smaller Reynolds numbers with appropriate annealing rates. In experimental observations this border depends, as we must expect, on the type of the disturbance; *Re* values between 1120 and 1480 have been reported. The calculations also shed further light on the mentioned relation between the turbulence onset and the existence of the unstable stationary states $\mathbf{w}(\mathbf{x})$ with finite $E_{\rm dist}(\mathbf{w})$ (cf. Sec. VIII). There are indications that turbulence can be maintained down to $Re=1000$, but that below this value the domain of attraction of the turbulent state is too small to be detectable. By this we mean that the subtle nonnormal-nonlinear mechanism is no longer successful, at least within the mode-number-reduced model. Incidentally, the Nagata-Clever-Busse state mentioned above exists for $Re\geqslant 500$ already.

X. SUMMARY

This Colloquium was devoted to drawing a physical picture of the mechanism which is responsible for the onset of turbulence despite (linear) stability of the laminar shear flow. Various approaches and notions have been advocated to solve this old problem: instability, subcritical transition, bistability, nonlinear instability, secondary instability, and growth by destabilization. Here I described and provided confirming arguments for a subtle mechanism of nonnormal growth of disturbances that have not yet adapted to the flow, and are rotated to become adapted, fit ones, complemented by their nonlinear interaction, which remixes and recreates misfit components anew. The mechanism cannot be understood in terms of the eigenvalues but rests on the bunching of a subset of eigenfunctions, induced by their coupling to the laminar flow advection. These are the main ingredients of an algebraically increasing and sustainedly fluctuating disturbance of the laminar flow, called turbulence.

Such an enterprise needs a large number of degrees of freedom. Various other notions of recent emphasis in stability analysis and pattern formation are not relevant to the problem. One has no eigenvalue instability, no bifurcation or period doubling, no center manifold theorem, no Landau-Hopf-Ruelle-Takens sequence 1-2-3-∞. All this has never been observed in various Couette or Poiseuille shear flows at the onset of turbulence. In contrast, the mechanism rests on the multiple effects of this absolutely unique convective nonlinearity $(\mathbf{u}\cdot\nabla)\mathbf{u}$: nonnormality, coupling to the energy supply, bunching of the disturbance eigenspace, proper remixing via quadratic interaction and comparison of the spatial vortex structure (probed by means of ∇) with the local flow direction.

Further elucidation, confirmation, explaining existing experimental observations, and useful application of the insights into this exciting mechanism of transition to turbulence are the challenge now.

ACKNOWLEDGMENTS

It is my sincere pleasure to acknowledge many stimulating conversations and suggestions for the manuscript by Ulrich Brosa, Bruno Eckhardt, Thomas Gebhardt, Martin Holthaus, Detlef Lohse, Itamar Procaccia, K. R. Sreenivasan, and many others.

REFERENCES

Baggett, J. S., and L. N. Trefethen, 1997, Phys. Fluids **9**, 1043–1052.

Bayly, B. J., S. A. Orszag, and T. Herbert, 1988, Annu. Rev. Fluid Mech. **20**, 359–391.

Benney, D. J., and L. H. Gustavson, 1981, Stud. Appl. Math. **64**, 185–209.

Boberg, L., and U. Brosa, 1988, Z. Naturforsch., A: Phys. Sci. **43**, 697–726.

Bottin, S., O. Dauchot, F. Daviaud, and P. Manneville, 1998, Phys. Fluids **10**, 2597–2607.

Brosa, U., 1989, J. Stat. Phys. **55**, 1303–1312.

Brosa, U., and S. Grossmann, 1999a, Eur. Phys. J. B **9**, 343–354.

Brosa, U. and S. Grossman, 1999b, "Hydrodynamic vector potentials," preprint, Marburg.

Butler, K. M., and B. F. Farrell, 1992, Phys. Fluids A **4**, 1637–1650.

Butler, K. M., and B. F. Farrell, 1993, Phys. Fluids A **5**, 774–777.

Chandrasekhar, S., 1961, *Hydrodynamic and Hydromagnetic Stability* (Clarendon, Oxford).

Chapman, S. J., 1999, "Subcritical transition in channel flows," preprint, Oxford.

Clever, R. M., and F. H. Busse, 1992, J. Fluid Mech. **234**, 511–527.
Clever, R. M., and F. H. Busse, 1997, J. Fluid Mech. **344**, 137–153.
Coles, D., 1965, J. Fluid Mech. **21**, 385–425.
Couette, M., 1890, Ann. Chim. Phys. **6**, 433–510.
Coullet, P., and J. Tresser, 1978, J. Phys. (Paris), Colloq. **39**, C5–C25.
Cvitanović, P., 1988, Phys. Rev. Lett. **61**, 2729–2732.
Darbyshire, A. G., and T. Mullin, 1995, J. Fluid Mech. **289**, 83–114.
Dauchot, O., and F. Daviaud, 1994, Europhys. Lett. **28**, 225–230.
Dauchot, O., and F. Daviaud, 1995, Phys. Fluids **7**, 335–343.
Drazin, P. G., and W. H. Reid, 1981, *Hydrodynamic Stability* (Cambridge University, Cambridge, England).
Eckhardt, B., 1999, private communication.
Eckhardt, B., and S. Grossmann, 1994, Phys. Rev. E **50**, 4571–4576.
Eckhardt, B., and G. Ott, 1994, Z. Phys. B: Condens. Matter **90**, 259–266.
Eckhardt, B., and A. Mersmann, 1999, Phys. Rev. E **60**, 509–517.
Eckhardt, B., K. Marzinzik, and A. Schmiegel, 1998, in *A Perspective Look at Nonlinear Media*, edited by J. Parisi, S. C. Müller, and W. Zimmermann, Lecture Notes in Physics, Vol. 503 (Springer, Berlin), pp. 327–338.
Eckmann, J.-P., and D. Ruelle, 1985, Rev. Mod. Phys. **57**, 617–656.
Esser, A., and S. Grossmann, 1996, Phys. Fluids **8**, 1814–1819.
Feigenbaum, M. J., 1978, J. Stat. Phys. **19**, 25–52.
Gebhardt, T., and S. Grossmann, 1993, Z. Phys. B: Condens. Matter **90**, 475–490.
Gebhardt, T., and S. Grossmann, 1994, Phys. Rev. E **50**, 3705–3711.
Gebhardt, T., and S. Grossmann, 1999, unpublished.
Grossmann, S., and S. Thomae, 1977, Z. Naturforsch. **32A**, 1353–1363.
Grossmann, S., 1994, in *Fundamental Problems in Statistical Mechanics VIII*, edited by H. van Beijeren and M. H. Ernst (North-Holland/Elsevier, Amsterdam), pp. 279–303.
Grossmann, S., 1995, Phys. Rev. E **51**, 6275–6277.
Gustavson, L. H., 1981, J. Fluid Mech. **112**, 253–264.
Gustavson, L. H., 1991, J. Fluid Mech. **224**, 241–260.
Hamilton, J. M., J. Kim, and F. Waleffe, 1995, J. Fluid Mech. **287**, 317–348.
Heisenberg, W., 1924, Ann. Phys. (Leipzig) **74**, 577–627.
Henningson, D. S., 1991, in *Advances in Turbulence*, edited by A. V. Johansson and P. H. Alfredsson (Springer, Berlin), pp. 279–284.
Henningson, D. S., A. Lundbladh, and A. V. Johansson, 1993, J. Fluid Mech. **250**, 169–207.
Herbert, T., 1988, Annu. Rev. Fluid Mech. **20**, 487–526.
Hopf, E., 1948, Commun. Pure Appl. Math. **1**, 308–322.
Joseph, D. D., 1976, *Stability of Fluid Motions I and II* (Springer, Berlin).
Kaplan, J. L., and J. A. Yorke, 1979, in *Functional Differential Equations and Approximation of Fixed Points*, edited by H.-O. Peitgen and H.-C. Walter, Lecture Notes in Mathematics Vol. 730 (Springer, Berlin), p. 204.
Landahl, M. T., 1980, J. Fluid Mech. **98**, 243–251.
Landau, L. D., 1944, C. R. (Dokl.) Acad. Sci. URSS **44**, 311–314.
Landau, L. D., and E. M. Lifschitz, 1991, *Lehrbuch der Theoretischen Physik*, Hydrodynamik Vol. 6 (Akademie, Berlin).
Lieb, E., 1984, Commun. Math. Phys. **92**, 473–480.
Lin, C. C., 1945a, Q. Appl. Math. **3**, 117–142.
Lin, C. C., 1945b, Q. Appl. Math. **3**, 218–234.
Lin, C. C., 1946, Q. Appl. Math. **4**, 277–301.
Lohse, D., 1994, Phys. Rev. Lett. **73**, 3223–3226.
Lundbladh, A., D. S. Henningson, and S. C. Reddy, 1993, *Threshold Amplitudes for Transition in Channel Flows*, Proceedings of the ICASE Workshop on Transition, Turbulence, and Combustion.
Monin, A. S., and A. M. Yaglom, 1999, *Statistical Fluid Mechanics, The Mechanics of Turbulence*, Vol. I, Chap. 4, New English Edition, revised, updated, and augmented by A. M. Yaglom, Center for Turbulence Research—CTR Monograph (Stanford University and NASA Ames Research Center).
Nagata, M., 1990, J. Fluid Mech. **217**, 519–527.
Nagata, M., 1997, Phys. Rev. E **55**, 2023–2025.
Nicodemus, R., S. Grossmann, and M. Holthaus, 1999, Eur. Phys. J. B **10**, 385–396.
Nishioka, M., S. Iida, and Y. Ishikawa, 1975, J. Fluid Mech. **72**, 731–751.
Orr, W. M. F., 1907, Proc. Irish Acad. **27**, 9–138.
Orszag, S. A., 1971, J. Fluid Mech. **50**, 689–703.
Orszag, S. A., and L. C. Kells, 1980, J. Fluid Mech. **96**, 161–205.
Orszag, S. A., and A. T. Patera, 1980, Phys. Rev. Lett. **45**, 989–993.
Orszag, S. A., and A. T. Patera, 1983, J. Fluid Mech. **128**, 347–385.
Pohl, R. W., 1962, *Einführung in die Physik I, Mechanik-Akustik-Wärmelehre* (Springer, Berlin), Sec. 90, Abb. 256*.
Rayleigh, Lord, 1880, Proc. London Math. Soc. **11**, 57–70.
Rayleigh, Lord, 1887, Proc. London Math. Soc. **19**, 67–73.
Rayleigh, Lord, 1916, Philos. Mag. **32**, 529–546.
Reddy, S. C., P. J. Schmid, and D. S. Henningson, 1993, SIAM (Soc. Ind. Appl. Math.) J. Appl. Math. **53**, 15–47.
Reddy, S. C., and D. Henningson, 1993a, J. Fluid Mech. **252**, 57–70.
Reddy, S. C., and D. Henningson, 1993b, J. Fluid Mech. **252**, 239–264.
Reddy, S. C., and D. Henningson, 1994, Phys. Fluids **6**, 1396–1398.
Reddy, S. C., P. J. Schmid, J. S. Baggett, and D. S. Henningson, 1998, J. Fluid Mech. **365**, 269–303.
Reynolds, O., 1883, Philos. Trans. R. Soc. London **174**, 935–982.
Ruelle, D., 1978, *Statistical Mechanics, Thermodynamic Formalism* (Addison-Wesley, Reading, MA).
Ruelle, D., 1982, Commun. Math. Phys. **87**, 287–302.
Ruelle, D., 1984, Commun. Math. Phys. **93**, 285–300.
Ruelle, D., and F. Takens, 1971, Commun. Math. Phys. **20**, 167–192.
Schlichting, H., 1959, in *Handbuch der Physik VIII/1* (Springer, Berlin), Figs. 1a, b.
Schmiegel, A., and B. Eckhardt, 1997, Phys. Rev. Lett. **79**, 5250–5253.
Schmiegel, A., and B. Eckhardt, 1999a, ''Dynamics of Perturbations in plane Couette flow,'' preprint, Marburg.
Schmiegel, A., and B. Eckhardt, 1999b, ''Sustained turbulence in annealed plane Couette flow,'' preprint, Marburg.
Sommerfeld, A., 1908, in *Proceedings of the 4th International Congress of Mathematicians, Rome*, Vol. III, pp. 116–124.

Taylor, G. I., 1923, Philos. Trans. R. Soc. London, Ser. A **223**, 289–343.
Tillmark, N., and P. H. Alfredsson, 1992, J. Fluid Mech. **235**, 89–102.
Thomson, Sir William, (Lord Kelvin), 1887, Philos. Mag. **24**, 188–196.
Trefethen, L. N., A. E. Trefethen, S. C. Reddy, and T. A. Driscol, 1993, Science **261**, 578–584.
Waleffe, F., 1995, Phys. Fluids **7**, 3060–3066.
Waleffe, F., J. Kim, and J. M. Hamilton, 1993, in *Turbulent Shear Flows 8*, edited by F. Durst *et al.* (Springer, Berlin), pp. 37–49.
Wygnanski, I. J., and F. H. Champagne, 1973, J. Fluid Mech. **59**, 281–335.